Spatially Discordant Alternans in Cardiac Tissue: Role of Calcium Cycling

Daisuke Sato, Yohannes Shiferaw, Alan Garfinkel, James N. Weiss, Zhilin Qu and Alain Karma

Circ. Res. 2006;99;520-527; originally published online Aug 10, 2006;
DOI: 10.1161/01.RES.0000240542.03986.e7
Circulation Research is published by the American Heart Association. 7272 Greenville Avenue, Dallas, TX 72514
 Print ISSN: 0009-7330. Online ISSN: 1524-4571

Spatially Discordant Alternans in Cardiac Tissue
Role of Calcium Cycling

Daisuke Sato,* Yohannes Shiferaw,* Alan Garfinkel, James N. Weiss, Zhilin Qu, Alain Karma

Abstract—Spatially discordant alternans, where the action potential duration (APD) and intracellular calcium transient (Ca_i) alternate with opposite phase in different regions of tissue, is known to promote wave break and reentry. However, this phenomenon is not completely understood. It is known that alternans at the cellular level can be caused by dynamical instabilities arising from either membrane voltage (V_m) attributable to steep APD restitution or to calcium (Ca) cycling. Here, we used a mathematical model of intracellular Ca cycling, coupled with membrane ion currents, to investigate the dynamics of V_m and Ca_i transient alternans in an isolated cell, in two electrotonically coupled cells, and in 1D spatially homogeneous tissue. Our main finding is a novel instability mechanism in which the bidirectional coupling of V_m and Ca_i can drive the Ca_i transient of two neighboring cells to be out of phase. This instability is manifested in cardiac tissue by the dynamical formation of spatially discordant alternans. In this case, Ca_i transient alternans can reverse phase over a length scale of one cell, whereas APD alternans reverses phase over a much longer length scale set by the electrotonic coupling. We analyze this mechanism in detail and show that it is a robust consequence of experimentally established properties of the bidirectional coupling between Ca cycling and V_m dynamics. Finally, we address the experimental relevance of these findings and suggest physiological conditions under which these patterns can be observed. **(*Circ Res*. 2006;99:520-527.)**

Key Words: discordant alternans ■ calcium cycling

Ventricular fibrillation (VF) is initiated when a propagating electrical wave fractionates as it passes over tissue with nonuniform electrophysiological properties. This dispersion of refractoriness has traditionally been attributed to the presence of fixed structural and electrical heterogeneities.[1,2] However, recent studies have shown that single-cell dynamics can play an important role in promoting VF.[3,4] In particular, alternans, a beat-to-beat alternation in the action potential duration (APD) at the single-cell level, can lead to the formation of spatially discordant alternans in tissue,[1,5–7] where regions of long–short APD alternation occur adjacent to regions with short–long APD alternation. This dynamical phenomenon is arrhythmogenic because it leads to the formation of steep gradients of refractoriness that can promote wave break and reentry.[1,2]

The mechanism underlying spatially discordant alternans is still not well understood. Pastore et al[1] have suggested that spatially discordant alternans is a consequence of fixed electrophysiological heterogeneity in cardiac tissue. On the other hand, theoretical studies have also shown that this phenomenon can occur in spatially homogeneous tissue[8–10] because of the interaction between APD alternans induced via a steep APD restitution curve and restitution of conduction velocity (CV). However, a further complexity in elucidating the mechanism of discordant alternans at a tissue level arises from the fact that, at the cellular level, APD alternans can be caused either by (1) A dynamical instability of V_m dynamics that is attributable to the gating kinetics of membrane ion channels that regulate V_m. Previous studies[3,11] have typically attributed alternans to gating kinetics that lead to a steep APD restitution curve; (2) Unstable intracellular Ca cycling, which in turn drives APD alternans via its effects on Ca-sensitive membrane currents.[12,13] Because V_m and Ca_i cycling are bidirectionally coupled, it is difficult to pinpoint which of these two possibilities is responsible for alternans. As a result, it is not known how the formation of discordant alternans in cardiac tissue depends on the cellular instability mechanism.

In this article, we apply mathematical modeling to test the hypothesis that discordant alternans in cardiac tissue can be initiated by a new mechanism that does not require CV restitution when alternans originate from a dynamical instability of calcium cycling. To test this hypothesis, we carry out simulations of V_m dynamics and Ca cycling in a cable of electrotonically coupled cells. The results demonstrate that

Original received December 8, 2005; revision received July 10, 2006; accepted August 1, 2006.

From the Department of Physics and Center for Interdisciplinary Research on Complex Systems (D.S., A.K.), Northeastern University, Boston, Mass; and Departments of Medicine (Cardiology) (Y.S., A.G., J.N.W., Z.Q.) and Physiology (A.G., J.N.W.), David Geffen School of Medicine at the University of California, Los Angeles.

*Both authors contributed equally to this study.

Correspondence to Dr Yohannes Shiferaw, Department of Cardiology, UCLA Cardiovascular Research Laboratory, 675 Charles E. Young Dr S, MRL 3645, Los Angeles, CA 90095. E-mail yshiferaw@mednet.ucla.edu

Circulation Research **is available at http://circres.ahajournals.org** **DOI: 10.1161/01.RES.0000240542.03986.e7**

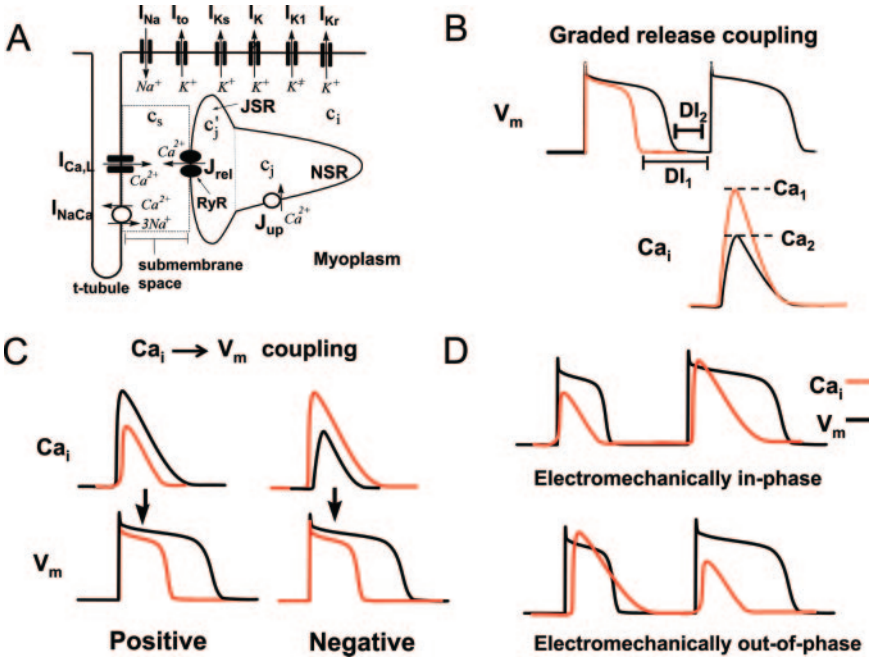

Figure 1. A, Illustration of the Ca_i cycling machinery and ionic currents implemented in the ionic model. B, Illustration of graded release coupling. The peak of the Ca_i transient at a given beat (lower trace) depends on the DI at the previous beat (upper trace). The DI influences the magnitude of the Ca current and hence the amount of Ca release at the next beat. Here, the peak of the Ca transient on the next beat, denoted by Ca_1 and Ca_2, corresponds to DI_1 and DI_2 respectively. C, Illustration of positive and negative $Ca_i \rightarrow V_m$ coupling. Positive (negative) coupling refers to the case when a large Ca_i transient at a given beat tends to prolong (shorten) the APD of that beat. D, Illustration of electromechanically in-phase and out-of-phase alternans during steady-state pacing.

discordant alternans can be formed, independently of CV restitution, when the Ca_i transient and APD of an isolated myocyte are electromechanically out of phase, ie, a large-small-large Ca_i transient corresponds to a short-long-short APD. Moreover, when the Ca_i transient and APD are in phase, sufficiently steep CV-restitution is required to initiate discordant alternans as shown in previous studies.[8–10] We explain these findings based on experimentally established properties of cardiac cells, and suggest experimental conditions under which this phenomenon can be observed.

Materials and Methods

Numerical Simulations

We modeled a 1D strand of homogeneous tissue using the cable equation:

$$\frac{\partial V}{\partial t} = -I_{ion}/C_m + D\frac{\partial^2 V}{\partial x^2} \quad (1)$$

where $C_m = 1\mu F/cm^2$ is the transmembrane capacitance, $D = 5\times10^{-4}$ cm^2/ms is the effective diffusion coefficient of membrane voltage in cardiac tissue, and where I_{ion} is the total ionic current density. The cable equation was integrated with an operator splitting method.[14] The space step was $\Delta x = 0.015$ cm, and the time step was adaptively varied between 0.01 ms and 0.1 ms. The ionic current was modeled by integrating a model of Ca cycling developed by Shiferaw et al.[13], coupled with the canine action potential model of Fox et al.[15] An illustration of the relevant ionic currents and Ca cycling machinery is shown in Figure 1A. Details of the mathematical formulation of the model are described in the online data supplement, available at http://circres.ahajournals.org. In addition, we modeled an isolated cell by integrating in time $dV/dt = -I_{ion}/C_m$, and two electrotonically coupled cells, with voltage V_1 in cell 1 and V_2 in cell 2, by integrating the two coupled equations $dV_1/dt = -I_{ion}/C_m + \kappa(V_2 - V_1)$ and $dV_2/dt = -I_{ion}/C_m + \kappa(V_1 - V_2)$ with a coupling strength $\kappa = D/\Delta x^2$.

Data Analysis

To determine the spatial distribution of Ca_i transient alternans, we computed the difference in the peak Ca_i transient from one beat to the next defined as:

$$\Delta Ca_i(x,n) = \frac{(-1)^n}{2} c_{n+1}(x) - c_n(x) \quad (2)$$

where n is the beat number, and $c_n(x)$ is the peak of the Ca_i transient measured at position x along the cable. The factor of $(-1)^n$ was introduced such that the amplitude of alternans does not change sign at every beat. The spatiotemporal evolution of Ca_i transient alternans was visualized by plotting $\Delta Ca_i(x,n)$. Likewise, the spatiotemporal distribution of APD alternans is measured using the quantity:

$$\Delta APD(x,n) = \frac{(-1)^n}{2}[\mathrm{APD}_{n+1}(x) - \mathrm{APD}_n(x)]. \quad (3)$$

With these definitions, the nodes separating spatially out-of-phase regions of Ca_i transient and APD alternans are located at the positions along the cable where $\Delta Ca_i(x,n) = 0$ and $\Delta APD(x,n) = 0$, respectively. Positive and negative values of ΔCa_i and ΔAPD on each side of these contours correspond to opposite phases of alternans.

Pacing Protocol

To study the dynamics of alternans, we paced an isolated cell, two coupled cells, and a 1D cable using a current stimulus of duration 1 ms and amplitude of 50 $\mu A/\mu F$. In the cable, we paced the left-most five cells to ensure propagation. In all cases, we applied a protocol where current was applied for 100 beats at a pacing cycle length (PCL) of 500 ms, after which the PCL was decreased by two ms every 50 beats. Following the method of Riccio et al,[16] we will refer to this protocol as the "dynamic pacing protocol."

Realistic Cell-to-Cell Fluctuations

Spatial and temporal heterogeneities are intrinsic properties of cardiac tissue. In this article, we model cell-to-cell variations by assuming that the constituents of all the cells are identical but taking into account the stochastic fluctuations of ion currents in the cell. In particular, we simulate the total current pumping Ca from the cytosol into the sarcoplasmic reticulum (SR), by modeling the stochastic properties of a finite number of SR Ca^{2+}-ATPase (SERCA) pumps. Our approach, following the method of Fox and Lu,[17] is to explicitly model the uptake current via a Langevin equation with a noise term that depends explicitly on the number of channels in the cell. Details of the current dynamics and noise formulation are given in the online data supplement.

Cellular Alternans and Bidirectional Coupling

In this work, we study the dynamics of alternans induced by unstable Ca cycling. Alternans is induced in our model by increasing the steepness, at high SR loads, of the function relating SR Ca release to SR Ca load, as described theoretically,[13,18] and experimentally by Diaz et al.[19] A key feature of the model is that when the cell is paced rapidly with a periodic AP clamp, Ca_i transient alternans develop,[13] as shown experimentally in isolated rabbit myocytes[12] and also in guinea pig myocytes.[20] Moreover, when the Ca_i transient alternates, APD alternates secondarily, because Ca_i affects ionic currents that regulate APD, primarily via the Na^+/Ca^{2+} exchanger and the L-type Ca current inactivation rate. Hereafter, we will refer to alternans induced via a steep SR Ca release-load gain as Ca-driven alternans.

The relationship between APD and Ca_i transient alternans in the single cell is dependent on the bidirectional coupling between Ca and V_m. First, let us consider how the Ca transient at a given beat is influenced by the membrane voltage. This coupling is determined by the well-established property of graded SR Ca release,[21–23] whereby the amount of SR Ca released is graded with respect to the whole cell L-type Ca current. The availability of the L-type Ca current at a given beat depends critically on the previous diastolic interval (DI). A larger DI gives more time for recovery of L-type Ca channels at the resting membrane potential. Thus, in our physiologically based cell model, graded release requires that the peak of the Ca_i transient increases in response to an increase of DI at the previous beat, as illustrated in Figure 1B. We refer to this relationship as graded release coupling. Note that although this coupling is typically observed in cardiac myocytes, other factors may override its effect. For example, I_{to} may shorten APD while, at the same time, increasing the driving force for early Ca entry via the L-type Ca current to potentate SR Ca release.[24,25] However, we did not study this case here.

Next, we consider the unidirectional coupling of Ca on V_m ($Ca_i \rightarrow V_m$ coupling). Two distinct cases can be distinguished. The first, referred to as positive $Ca_i \rightarrow V_m$ coupling, illustrated in Figure 1C, corresponds to the case in which an increase in the peak Ca_i transient amplitude lengthens the APD. The second, referred to as negative $Ca_i \rightarrow V_m$ coupling (Figure 1C), corresponds to the case in which an increase in the peak Ca_i transient amplitude shortens the APD. Both the sign and the magnitude of the coupling is dictated by the relative contributions of the L-type Ca current and the Na^+/Ca^{2+} exchange current to APD. A larger Ca_i transient tends to inactivate the whole cell L-type Ca current more rapidly via Ca-induced inactivation, which tends to shorten the APD. However, a large Ca_i transient concomitantly increases the net inward current from electrogenic Na^+/Ca^{2+} exchange, which tends to prolong APD. The $Ca_i \rightarrow V_m$ coupling was varied in our ionic model by changing the degree of Ca-induced inactivation of the L-type Ca current, as described in the online data supplement.

Electromechanically In-Phase and Out-of-Phase Alternans

The bidirectional coupling between the APD and the Ca_i transient determines the relative phase of APD and Ca_i transient alternans during steady-state pacing.[26–28] For Ca-driven alternans, positive $Ca_i \rightarrow V_m$ coupling always leads to electromechanically in-phase alternans, as illustrated in Figure 1D, where a long–short–long APD pattern corresponds to a large-small-large Ca_i transient. In contrast, negative $Ca_i \rightarrow V_m$ leads to electromechanically out-of-phase alternans (Figure 1D), where a long–short–long APD corresponds to a small–large–small Ca_i transient. When alternans are attributable to an instability of V_m dynamics, steady-state electromechanical alternans are always in phase. This is because, in this case, the Ca_i transient is slaved to V_m via the graded release coupling (Figure 1B), so that Ca_i transient alternans is always in phase with APD alternans.

Results

Synchronization and Desynchronization of Two Coupled Cells

In this section, we study systematically the relationship between $Ca_i \rightarrow V_m$ coupling and Ca transient alternans, for the case when alternans are attributable to unstable Ca cycling. As a starting point, we first consider a simple system of two electrotonically coupled cells, with the main result that two cells alternate out of phase because of an intrinsic dynamical instability when the $Ca_i \rightarrow V_m$ coupling is negative. We then study the case of a cable of several hundred cells to show that the same instability mechanism leads to spatially discordant alternans that are formed independently of CV restitution.

Single-Cell Alternans

As a starting point, we first plotted the amplitude of APD alternans (ΔAPD) and Ca_i transient alternans (ΔCa_i) as a function of PCL, for an isolated cell paced using the dynamic pacing protocol. The amplitude of alternans is measured after steady state is reached, using the 49th and 50th beats at each PCL. We considered both positive (Figure 2A) and negative (Figure 2B) $Ca_i \rightarrow V_m$ coupling by adjusting the inactivation kinetics of the L-type Ca current, as described in the online supplement. As shown in Figure 2A, for positive $Ca_i \rightarrow V_m$ coupling, alternans onset occurred at PCL=315 ms and APD alternans was in phase with Ca_i transient alternans, ie, ΔAPD and ΔCa_i always had the same sign after the bifurcation to alternans (electromechanically in phase). On the other hand, for the negative $Ca_i \rightarrow V_m$ coupling parameters, alternans onset was at PCL=340 ms, and once alternans developed, ΔAPD always had an opposite sign compared with ΔCa_i (electromechanically out of phase).

Two Coupled Cells

We then paced two electrotonically coupled cells with the same model parameters used in the single-cell simulations. Here, both cells had identical parameters but differed only by small ($\approx$0.1%) stochastic fluctuations in the intracellular Ca cycling dynamics. Fluctuations were incorporated as described in the methods section. In Figure 2C we show the amplitude of alternans for both cells as a function of pacing rate for the case of positive $Ca_i \rightarrow V_m$ coupling ie, same model parameters as used in Figure 2A. As shown, alternans onset occurs at the same pacing rate as the single-cell case (PCL=315 ms), and alternans phase is synchronized, ie, ΔAPD and ΔCa_i had the same sign in cell 1 and cell 2. In Figure 2D, we applied the dynamic pacing protocol to a pair of cells with negative $Ca_i \rightarrow V_m$ coupling ie, same model parameters as in Figure 2B. As shown, Ca_i transient alternans occurred simultaneously in both cells at a PCL=355 ms (indicated by the vertical green line), which is earlier than the onset of alternans for the single cell (vertical black line). Also, APD alternans were not observed in both cells. Furthermore, Ca_i transient alternans in cell 1 and cell 2 are out of phase. That is, ΔCa_i is positive in cell 1 and negative in cell 2, as shown. Moreover, despite the significant degree of Ca_i transient alternans, APD did not alternate in either cell. This effect is attributable to electrotonic interaction between the two cells, such that the APD shortening effect of a large Ca_i transient in one cell was balanced by the APD prolonging effect of the opposite phase small Ca_i transient in the other cell.

Formation of Spatially Discordant Alternans in a Cable of Many Cells

The simplified system studied above illustrates the rich dynamical behavior that can arise by coupling two cardiac

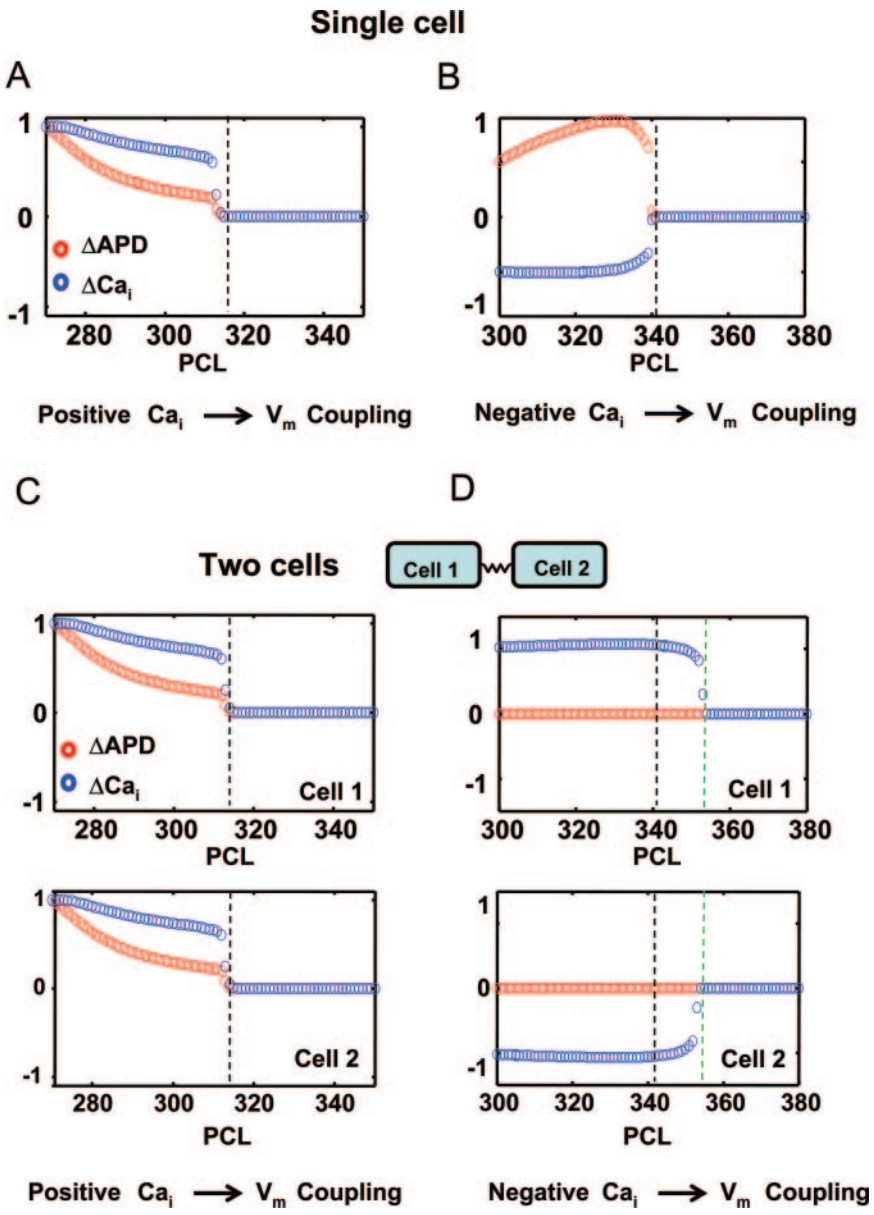

Figure 2. Alternans dynamics during the dynamic pacing protocol. A, Steady-state normalized amplitude of APD (ΔAPD) and Ca_i transient (ΔCa_i) alternans as a function of PCL for an isolated cardiac cell paced using the dynamic pacing protocol. Here, the amplitude of alternans is normalized to the maximum value. The cell model is adjusted so that the $Ca_i \rightarrow V_m$ coupling is positive. Here, alternans amplitude is measured by subtracting the APD and peak Ca_i at the 50th and 49th beats at the given PCL. The onset of alternans is denoted by the vertical dashed line. B, Same simulation as in A using cell model parameters with negative $Ca_i \rightarrow V_m$ coupling. C, Amplitude of alternans within two electrotonically paced cardiac cells. Here, the cell model used is the same as in A. D, Same simulation as in C, using the same model parameters as in B. Notice that the onset of alternans (vertical green line) occurs at an earlier PCL than in the isolated cell (vertical black line).

cells. Here, we study the case of a cable of many cells (200 cells) that is paced at 1 end. For the case of positive $Ca_i \rightarrow V_m$ coupling, Figure 3A through 3C shows the steady-state spatial distribution of both ΔAPD and ΔCa_i at 3 different PCLs. As shown, alternans was spatially synchronized at PCL=310 ms. However, at a more rapid stimulation rate (PCL=280 ms), spatially discordant alternans formed spontaneously. In this case, both Ca and APD alternans were electromechanically in phase for all cells along the cable but reversed phase spatially at a node along the cable.

As shown in Figure 3D through 3F, we repeated the above simulation with negative $Ca_i \rightarrow V_m$ coupling parameters. Alternans amplitude was 0 across the cable at a PCL of 400 ms, but as the PCL was gradually shortened to 340 ms, spatially discordant alternans of the Ca_i transient and APD gradually grew from the spatially homogeneous state. The spatial pattern of alternans is characterized by the presence of many (>30) ΔCa_i nodes and a few APD nodes. We repeated the dynamic simulation protocol 16 times and found that the average spacing between ΔCa_i nodes, at PCL=340 ms, was roughly 0.045±0.004 cm, whereas the average spacing of ΔAPD nodes was 0.6±0.1 cm.

Role of Conduction Velocity Restitution

To uncover the mechanism that leads to the formation of spatially discordant alternans, we also computed the spatial distribution of CV during the discordant alternans patterns shown in Figure 3C and 3F. Figure 4A shows the spatial distribution of CV along the cable during the steady-state pattern shown in Figure 3C. Here, the dashed/solid line corresponds to CV along the cable for the 49th/50th paced beat. As shown, the CV of the pulse changed by roughly 2 cm/ms as it traveled down the cable. Figure 4B shows the CV restitution curve computed for the model. The two vertical dashed lines mark the range of DI engaged along the cable. Figure 4C shows the spatial distribution of CV during the

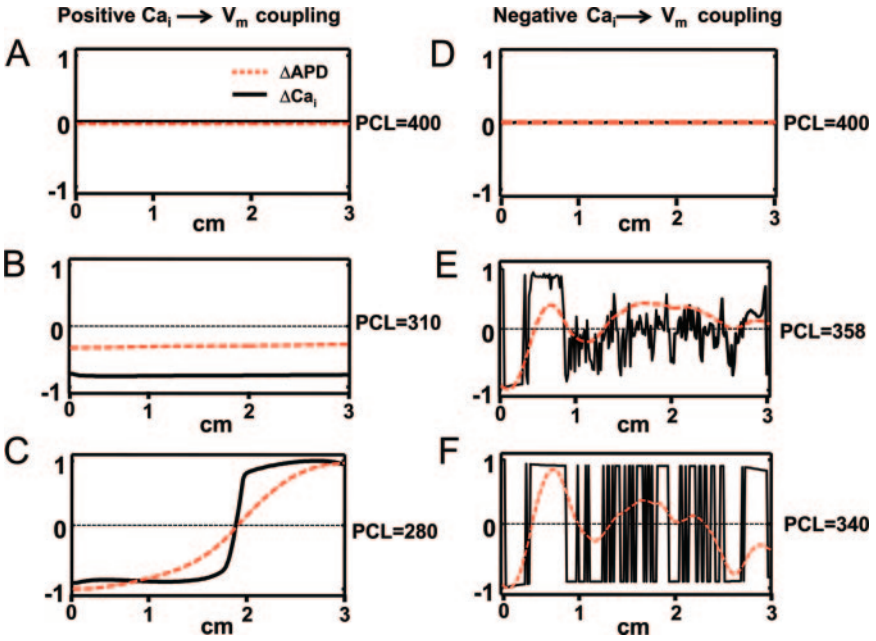

Figure 3. Distribution of Ca_i transient and APD alternans amplitude along a cable of cells with the same model parameters as in Figure 2A (positive $Ca_i \rightarrow V_m$ coupling). During the dynamic pacing protocol alternans amplitude was measured for each cell by computing ΔCa_i and ΔAPD from the 49th and 50th beats at PCL=400 ms (A), PCL=310 ms (B), and PCL=280 ms (C). D through F, Same simulation using the model parameters used in Figure 2B (negative $Ca_i \rightarrow V_m$ coupling) for PCL=400, 358, 340 ms. In all graphs, ΔCa_i and ΔAPD are normalized to the maximum value observed during the dynamic pacing protocol.

alternans pattern shown in Figure 3F. In this case, CV did not vary along the cable during discordant alternans. We also plotted the maximum range of DI engaged and found that indeed CV restitution was flat over the range of DIs engaged at that pacing rate (PCL=340 ms).

Discussion

$Ca_i \rightarrow V_m$ Coupling Determines the Relative Synchrony of Two Coupled Cells

The main finding of this work is that the bidirectional coupling between Ca_i and V_m dictates whether two coupled cells are synchronized or desynchronized. In particular, we find that if the $Ca_i \rightarrow V_m$ coupling is positive, such that alternans at the single-cell level is electromechanically in phase, then Ca_i transient alternans in neighboring cells will synchronize. On the other hand, if the $Ca_i \rightarrow V_m$ coupling is negative such that single-cell alternans is electromechanically out of phase, then Ca_i transient alternans desynchronize.

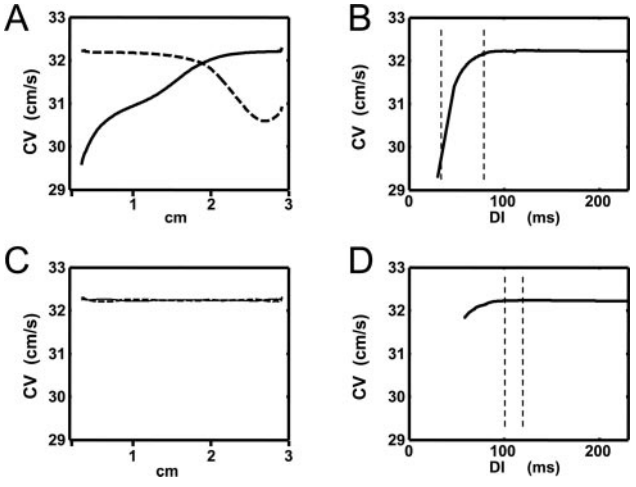

Figure 4. CV during discordant alternans. A, CV computed for the 49th (dashed line) and 50th (solid line) paced beats at PCL=280 ms, during the same simulation shown in Figure 3C. B, CV restitution curve for the ionic model parameters used in Figure 3C. The vertical dashed lines marks the maximum range of DI engaged along the cable during the 50th beat. C, CV measured along the cable for the 2 beats used to compute Figure 3F. D, CV restitution curve for the model parameters used in Figure 3F. Again, the dashed lines denote the range of DI engaged during the discordant alternans pattern shown in Figure 3F.

Mechanistic Explanation of Desynchronization Mechanism

To understand the mechanism for desynchronization, we analyze how $Ca_i \rightarrow V_m$ coupling, along with electrotonic coupling, dictates the evolution of Ca_i alternans. In Figure 5A, we illustrate the V_m and Ca_i transients of two independent cells

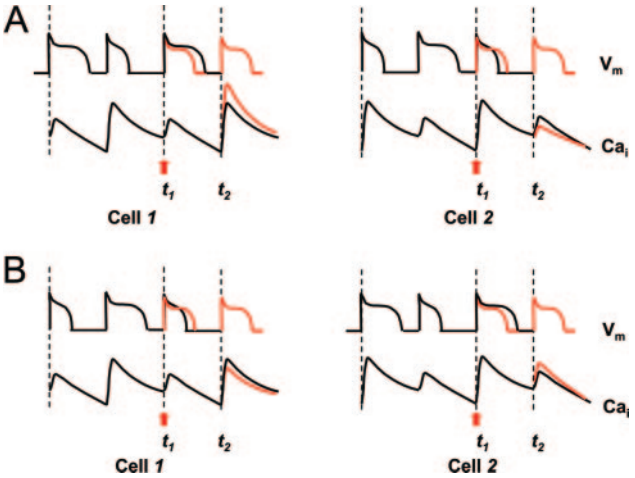

Figure 5. Schematic illustration of the desynchronization/synchronization mechanism when single-cell alternans are electromechanically in phase and out of phase. A, V_m and Ca_i vs time for neighboring cells 1 and 2 with negative $Ca_i \rightarrow V_m$ coupling. The cells are uncoupled before time t_1, after which they are coupled electrotonically. The red line denotes the time evolution after electrotonic coupling at time t_1. B, Same illustration as A with positive $Ca_i \rightarrow V_m$ coupling.

(cell 1 and cell 2) that are out of phase and which are then electrotonically coupled at time t_1. Here, we assume negative $Ca_i \rightarrow V_m$ coupling so that alternans is electromechanically discordant in both cells. The black and red lines depict schematically the time evolution of V_m and Ca_i in the absence and in the presence of electrotonic coupling, respectively. Two key factors determine the subsequent evolution of alternans:

***Electrotonic Coupling of* V_m**

This effect is illustrated with the red V_m traces after time t_1. Here, electronic coupling simply averages the APD of the 2 cells, thereby forcing them to have an identical V_m time course. Thus, the APD in cell 1 and cell 2 shorten and lengthen, respectively, in comparison with the APD that would have occurred if the 2 cells were not coupled.

Graded Release Coupling

The change in APD between times t_1 and t_2 will influence the amount of Ca release at time t_2 (the next beat) via the graded release coupling illustrated in Figure 1B. Hence, the large DI in cell 1 will lead to a larger Ca release on the next beat, whereas the smaller DI in cell 2 will yield a smaller Ca release. Note that APD shortening/lengthening will change the Ca influx into the cell and thus influence the amount of Ca released. However, we find that this effect is much smaller than that induced by graded release coupling because the change in SR load over 1 beat, caused by the change in APD, is relatively small in the present model.

The combined effects of 1 and 2 above is to cause the Ca_i transient of cell 1 and cell 2 to be more markedly different on the next beat, ie, the large release is larger, whereas the small release is smaller. Hence, the difference in phase of Ca_i transient alternans in the two neighboring cells is amplified from one beat to the next. This mechanism explains why the two coupled cells in our simulations exhibited out-of-phase Ca_i transient alternans during dynamic pacing. There, even very small differences in alternans phase, caused by stochastic fluctuations in Ca cycling properties, are amplified from beat to beat so that Ca_i transient alternans are forced to alternate with opposite phase. Hence, even though all cells in the cable have identical ionic properties, small ($<0.1\%$) stochastic differences are amplified dynamically by the above mechanism, to yield spatially discordant patterns after many beats.

On the other hand, in the case of positive $Ca_i \rightarrow V_m$ coupling, where alternans are electromechanically in phase, applying the same arguments given above shows that Ca_i transient alternans in neighboring cells (Figure 5B) tend to synchronize. Hence, in this case, small cell-to-cell differences between neighboring cells are diminished from beat to beat to yield spatially concordant alternans. In this case, steep CV restitution must be invoked to induce spatially discordant alternans via a different mechanism.

Initiation of Spatially Discordant Alternans in Homogeneous Tissue

When the $Ca_i \rightarrow V_m$ coupling is positive, spatially discordant alternans form only when CV alternates from beat to beat, ie, discordant alternans are associated with substantial CV variation along the cable. This mechanism for the induction of spatially discordant alternans is well known and has been extensively studied.[8–10] In these studies, it was shown that discordant alternans form in homogeneous tissue because of the interaction between APD alternans, induced via a steep APD restitution curve, and CV restitution. Similarly here, the same interaction between APD alternans and steep CV restitution suffices to initiate spatially discordant alternans in homogeneous tissue for short enough PCL. The main difference is that the APD alternans are driven by Ca_i alternans, which are attributable to an instability of Ca cycling, instead of an instability of V_m dynamics.

In the case of negative $Ca_i \rightarrow V_m$ coupling, we find that Ca_i transient alternans form into discordant patterns with many out-of-phase regions in the cable. These patterns were not dictated by CV restitution because the measured variations of CV along the cable were negligible. In this case, the spatial patterns are formed by the same mechanism that drives the Ca_i transient of 2 neighboring cells out of phase. That is, small cell-to-cell differences are amplified from beat to beat by the desynchronization effect of negative bidirectional coupling of V_m and Ca_i. Hence, arbitrarily small stochastic fluctuations grow and develop into spatially discordant alternans were the Ca_i transient of neighboring cells can alternate out of phase. The consequences of this desynchronization mechanism on subcellular scales, where Ca diffusion needs to be taken into account, has been the subject of a recent theoretical study.[29]

Spatial Scale of Discordant Alternans in Homogeneous Tissue

A major difference between positive and negative $Ca_i \rightarrow V_m$ coupling is the spacing between nodes of Ca alternans. For positive $Ca_i \rightarrow V_m$ coupling, we find that the spacing between nodes is on a tissue scale ($\approx$1 cm). In contrast, for negative $Ca_i \rightarrow V_m$ coupling, the spacing between nodes can range from 1 to a few cell lengths (100 to 400 μm). This short scale originates from the fact that the instability mechanism that drives discordant alternans in a cable of coupled cells is similar to the aforementioned instability mechanism that drives out-of-phase alternans in two electrotonically coupled identical cells. The tissue case is more complex, however, because several instability modes with different length scales can be manifested, with the spacing between nodes varying from 1 to several cells.

The difference between positive and negative $Ca_i \rightarrow V_m$ coupling is also reflected in the relationship between Ca and APD alternans patterns. For positive coupling, the nodes of V_m and Ca alternans essentially coincide. In contrast, for negative coupling, the spacing between nodes of APD alternans is substantially larger than the cellular-scale spacing between nodes of Ca alternans. The reason is that the diffusion constant of V_m in homogeneous tissue ($\approx$ 1 cm^2/sec) is at least 5 orders of magnitude larger than the molecular diffusion constant of Ca^{2+} ions (within the myoplasm and across gap junctions). Therefore, on the time scale of one APD, V_m diffuses on a spatial scale $\sqrt{D \times APD}$ of a few millimeters,[10] whereas Ca diffuses at most by a fraction of a cell length. Because APD alternans must be in phase within a

region of a size comparable to the diffusion scale of V_m, this tissue scale sets the spacing between nodes of APD alternans.

Robustness of the Simulation Findings

To what extent do the simulation findings depend on the detailed formulation of the ionic model[13,15] used in the present study? To answer this question, it is necessary to outline the essential physiological ingredients that underlie the desynchronization mechanism illustrated in Figure 5A. There are two essential conditions:

Alternans at the Single-Cell Level Must Be Attributable to a Dynamical Instability of Ca Cycling

This is an essential requirement because Ca_i transient alternans must not be slaved to APD alternans to be able to desynchronize on a cellular scale and hence must not originate from an instability of V_m dynamics. If the latter is true, graded release coupling ensures that Ca_i transient alternans are always electromechanically in phase with APD alternans.

$Ca_i \rightarrow V_m$ Coupling Must Be Negative

This is the crucial requirement that ensures that Ca cycling alternans drive electromechanically out-of-phase APD alternans, so that the arguments illustrated in Figure 5A can be applied. Here, the important feature is that a large Ca_i transient shortens the APD at the same beat. In this case, if alternans are attributable to unstable Ca cycling, a large-small-large Ca_i transient is always associated with a short–long–short APD.

We expect our findings to be robust in that any detailed ionic model that satisfies these conditions should exhibit qualitatively similar patterns of alternans as in the present simulations. This robustness, however, does not preclude the fact that the above conditions could in general be fulfilled by different ionic mechanisms.

Concluding Remarks

To test experimentally the novel predictions of this study, it is necessary to identify cardiac cells in which alternans are electromechanically out of phase. Our main prediction is that if a tissue of these cells is paced into alternans, then spatially discordant alternans should organize into complex spatiotemporal patterns similar to those shown in Figure 3E and 3F. A crucial feature of these patterns is that Ca_i transient alternans can form discordant patterns on the cellular scale, whereas APD alternans vary over a much larger length scale. In contrast, if Ca and APD are electromechanically in phase, then the spatial distribution of Ca alternans will be similar to that of APD alternans.

From the experimental stand point both in-phase and out-of-phase electromechanical alternans have been observed[12,28,30,31] in different cell types and under a variety of experimental conditions. For example, in rabbit cardiac myocytes alternans are consistently electromechanically in phase,[12,32] whereas in cat atrial myocytes alternans have been observed to be electromechanically out of phase.[33] Also, electromechanically out-of-phase alternans have been observed under ischemic conditions.[30] Furthermore, an interesting experimental study by Rubenstein et al[31] has shown that in isolated cat ventricular myocytes that at 36°C, APD alternates in phase with contraction, which mirrors the amplitude of the Ca_i transient, whereas at 32°C, they become out of phase. These observations suggest that the bidirectional coupling between V_m and Ca can vary with cell type and can be modulated by changing experimental conditions.

The possibility of observing Ca nodes with a spacing comparable to a cell length is consistent with experimental studies that demonstrate that subcellular Ca alternans can be spatially discordant within a single cell. For example, Kockskamper et al[34] imaged subcellular Ca in cat atrial cells and found that half of the cell could alternate out of phase with the other half. Also, Diaz et al[35] have shown subcellular discordant alternans in rat myocytes paced with a clamped AP waveform. These studies demonstrate that Ca alternans can change phase over subcellular length scales, much shorter than the diffusive length scale of V_m.

Sources of Funding

This study was supported by NIH/National Heart, Lung, and Blood Institute grants P50 HL52319 and P01 HL078931 and the Laubisch and Kawata Endowments.

Disclosures

None.

References

1. Pastore JM, Girouard SD, Laurita KR, Akar FG, Rosenbaum DS. Mechanism linking T-wave alternans to the genesis of cardiac fibrillation. *Circulation*. 1999;99:1385–1394.
2. Pastore JM, Rosenbaum DS. Role of structural barriers in the mechanism of alternans-induced reentry. *Circ Res*. 2000;87:1157–1163.
3. Karma A. Electrical alternans and spiral wave breakup in cardiac tissue. *Chaos*. 1994;4:461–472.
4. Garfinkel A, Kim YH, Voroshilovsky O, Qu Z, Kil JR, Lee MH, Karagueuzian HS, Weiss JN, Chen PS. Preventing ventricular fibrillation by flattening cardiac restitution. *Proc Natl Acad Sci U S A*. 2000;97:6061–6066.
5. Clusin WT. Calcium and cardiac arrhythmias: DADs, EADs, and alternans. *Crit Rev Clin Lab Sci*. 2003;40:337–375.
6. Qian YW, Clusin WT, Lin SF, Han J, Sung RJ. Spatial heterogeneity of calcium transient alternans during the early phase of myocardial ischemia in the blood-perfused rabbit heart. *Circulation*. 2001;104:2082–2087.
7. Pruvot EJ, Katra RP, Rosenbaum DS, Laurita KR. Role of calcium cycling versus restitution in the mechanism of repolarization alternans. *Circ Res*. 2004;94:1083–1090.
8. Qu Z, Garfinkel A, Chen PS, Weiss JN. Mechanisms of discordant alternans and induction of reentry in simulated cardiac tissue. *Circulation*. 2000;102:1664–1670.
9. Watanabe MA, Fenton FH, Evans SJ, Hastings HM, Karma A. Mechanisms for discordant alternans. *J Cardiovasc Electrophysiol*. 2001;12:196–206.
10. Echebarria B, Karma A. Instability and spatiotemporal dynamics of alternans in paced cardiac tissue. *Phys Rev Lett*. 2002;88:208101.
11. Nolasco JB, Dahlen RW. A graphic method for the study of alternation in cardiac action potentials. *J Appl Physiol*. 1968;25:191–196.
12. Chudin E, Goldhaber J, Garfinkel A, Weiss J, Kogan B. Intracellular Ca(2+) dynamics and the stability of ventricular tachycardia. *Biophys J*. 1999;77:2930–2941.
13. Shiferaw Y, Watanabe MA, Garfinkel A, Weiss JN, Karma A. Model of intracellular calcium cycling in ventricular myocytes. *Biophys J*. 2003;85:3666–3686.
14. Qu Z, Garfinkel A. An advanced algorithm for solving partial differential equation in cardiac conduction. *IEEE Trans Biomed Eng*. 1999;46:1166–1168.
15. Fox JJ, McHarg JL, Gilmour RF Jr. Ionic mechanism of electrical alternans. *Am J Physiol Heart Circ Physiol*. 2002;282:H516–H530.
16. Riccio ML, Koller ML, Gilmour RF Jr. Electrical restitution and spatiotemporal organization during ventricular fibrillation. *Circ Res*. 1999;84:955–963.

17. Fox RF, Lu Y. Emergent collective behavior in large numbers of globally coupled independently stochastic ion channels. *Phys Rev E Stat Phys Plasmas Fluids Relat Interdiscip Topics*. 1994;49:3421–3431.
18. Eisner DA, Choi HS, Diaz ME, O'Neill SC, Trafford AW. Integrative analysis of calcium cycling in cardiac muscle. *Circ Res*. 2000;87: 1087–1094.
19. Diaz ME, O'Neill SC, Eisner DA. Sarcoplasmic reticulum calcium content fluctuation is the key to cardiac alternans. *Circ Res*. 2004;94: 650–656.
20. Wan X, Laurita KR, Pruvot EJ, Rosenbaum DS. Molecular correlates of repolarization alternans in cardiac myocytes. *J Mol Cell Cardiol*. 2005; 39:419–428.
21. Bers DM. Cardiac excitation-contraction coupling. *Nature*. 2002;415: 198–205.
22. Wier WG, Egan TM, Lopez-Lopez JR, Balke CW. Local control of excitation-contraction coupling in rat heart cells. *J Physiol*. 1994;474: 463–471.
23. Bers DM. *Excitation-Contraction Coupling and Cardiac Contractile Force.* Boston, Mass: Kluwer; 2001.
24. Sah R, Ramirez RJ, Oudit GY, Gidrewicz D, Trivieri MG, Zobel C, Backx PH. Regulation of cardiac excitation-contraction coupling by action potential repolarization: role of the transient outward potassium current (I(to)). *J Physiol*. 2003;546:5–18.
25. Harris DM, Mills GD, Chen X, Kubo H, Berretta RM, Votaw VS, Santana LF, Houser SR. Alterations in early action potential repolarization causes localized failure of sarcoplasmic reticulum Ca2+ release. *Circ Res*. 2005;96:543–550.
26. Shiferaw Y, Sato D, Karma A. Coupled dynamics of voltage and calcium in paced cardiac cells. *Phys Rev E Stat Nonlin Soft Matter Phys*. 2005; 71:021903.
27. Walker ML, Rosenbaum DS. Repolarization alternans: implications for the mechanism and prevention of sudden cardiac death. *Cardiovasc Res*. 2003;57:599–614.
28. Euler DE. Cardiac alternans: mechanisms and pathophysiological significance. *Cardiovasc Res*. 1999;42:583–590.
29. Shiferaw Y, Karma A. Turing instability mediated by voltage and calcium diffusion in paced cardiac cells. *Proc Natl Acad Sci U S A*. 2006;103: 5670–5675.
30. Murphy CF, Horner SM, Dick DJ, Coen B, Lab MJ. Electrical alternans and the onset of rate-induced pulsus alternans during acute regional ischaemia in the anaesthetised pig heart. *Cardiovasc Res*. 1996;32: 138–147.
31. Rubenstein DS, Lipsius SL. Premature beats elicit a phase reversal of mechanoelectrical alternans in cat ventricular myocytes. A possible mechanism for reentrant arrhythmias. *Circulation*. 1995;91:201–214.
32. Goldhaber JI, Xie LH, Duong T, Motter C, Khuu K, Weiss JN. Action potential duration restitution and alternans in rabbit ventricular myocytes: the key role of intracellular calcium cycling. *Circ Res*. 2005;96:459–466.
33. Huser J, Wang YG, Sheehan KA, Cifuentes F, Lipsius SL, Blatter LA. Functional coupling between glycolysis and excitation-contraction coupling underlies alternans in cat heart cells. *J Physiol*. 2000;524(pt 3):795–806.
34. Kockskamper J, Blatter LA. Subcellular Ca2+ alternans represents a novel mechanism for the generation of arrhythmogenic Ca2+ waves in cat atrial myocytes. *J Physiol*. 2002;545:65–79.
35. Diaz ME, Eisner DA, O'Neill SC. Depressed ryanodine receptor activity increases variability and duration of the systolic Ca2+ transient in rat ventricular myocytes. *Circ Res*. 2002;91:585–593.